

Non-Metallic Material Science

Volume 2 | Issue 1 | 2020 April | ISSN 2661-3301 (Online)



Editor-in-Chief

Dr. Ali Durmus

Istanbul University Cerrahpasa, Turkey

Editorial Board Members

- | | |
|--|---|
| Ali Solati, Iran | Amid Ranjkesh, Korea |
| Lijian Meng, Portugal | Ning Luo, China |
| Edwin Peng, United States | Kotari Srinivasarao, India |
| Praveen Malik, India | Mostafa Ragab Abd El Wahab, Egypt |
| Sofyan A. Taya, Palestinian | N. Jeyaprakash, Taiwan |
| Hussein Mohammed Ali Ibraheem, Iraq | Antonio Bastos Pereira, Portugal |
| Samuel Paul David, Czech Republic | G. Udhaya Sankar, India |
| Hongyu Liu, China | Alexander Pyatenko, Japan |
| Sayed Faheem Naqvi, India | Andreas Rosenkranz, Germany |
| Dan Dobrotă, Romania | Ashok Panchapakesan, India |
| Manawwer Alam, Saudi Arabia | Zhongchang Wang, Portugal |
| Nasrin Oroujzadeh, Iran | Lei Zhai, United States |
| Nikolai Stoyanov Boshkov, Bulgaria | Laifa Shen, Germany |
| Alisa Buchman, Israel | Noel Ibrahim Akos, Nigeria |
| Yuhuan Fei, China | Chih-Ta Tsai, Taiwan |
| Jasbeer Singh Satwant Singh Sidhu, India | Moonis Ali Khan, Saudi Arabia |
| Chol-Hyon Kim, Korea | Hongyang Ma, China |
| Shivani Dhall, India | Upenyu Guyo, Zimbabwe |
| Mallinath Shrimanth Birajdar, India | Soumya Mukherjee, India |
| Azam Sobhani, Iran | Muhammad Imran Rashid, Pakistan |
| Yunyan Zhang, United Kingdom | Cheng-Fu Yang, Taiwan |
| Prabakaran M P, India | Miaoxiang Chen, Sweden |
| Nastaran Parsafard, Iran | Ana Queirós Barbosa, Portugal |
| Mohammad Sirousazar, Iran | Sikiru Oluwarotimi Ismail, United Kingdom |
| Suha K. Shihab, Iraq | Mohammad Rashed Iqbal Faruque, Malaysia |
| Kishore Debnath, India | Saeed Zeinali Heris, Iran |
| Hong-Liang Dai, China | Jelena Dragoslav Jovanovic, Serbia |
| Tao Huang, United States | Jean-Paul Moshe Lellouche, Israel |
| Shoujun Wu, China | Zilong Zhao, China |
| Amjad Khabaz, Turkey | Guoquan Nie, China |
| Linda Aissani, Algeria | Aline Teixeira de Souza, Brazil |
| Seifollah Jamalpour, Iran | Fellah Mammoun, Algeria |
| Emad Mohamed M. Ewais, Egypt | Ahmad Ali Mousa, Jordan |
| Marco Vinicius Chaud, Brazil | Nourredine AïT Hocine, France |
| Samson Jerold Samuel Chelladurai, India | Umberto Prisco, Italy |
| Nasser Sepehri Javan, Iran | Hoejin Kim, University of Texas |
| Prabhakaran Subramaniyan, France | Srijita Bharti, India |
| Padmanabhan Krishnan, India | Stefania Pasquale, Italy |
| Pradeep Lancy Menezes, United States | Rouholah Ashiri, Iran |
| Sivakumar Dhar Malingam, Malaysia | Ning Wu, China |
| Sina Matavos-Aramyan, Iran | Shen Liu, China |
| Arafa Hussien Aly, Egypt | Morteza Ehsani, Iran |
| Mohammad Farooq Wani, India | Anshu Sharma, India |
| Rishi Kumar, India | Chul Ho Park, Korea |
| Sourav Kundu, India | Hamid Reza Taghiyari, Iran |
| Ravi Shanker Vidyarthi, India | Latefa Sail, Algeria |

Volume 2 Issue 1 • April 2020 • ISSN 2661-3301 (Online)

Non-Metallic Material Science

Editor-in-Chief
Dr. Ali Durmus



**BILINGUAL
PUBLISHING CO.**
Pioneer of Global Academics Since 1984

Contents

Article

- 1 Solving the Problem of Silicon Dioxide Melting Based on Deviation Model**
Yuhan Sun Na Huang Jie Yu
- 6 Effects of Polypyrrole / Graphene Oxide Composites with Different Reaction Times on Electrochemical Performance**
Minzhen Feng Wei Lu Ranran Zhen Ya Wang Yun Zhou
- 9 Bio-fuel Production From Carbondioxide Gas Using *S. elongatus* PCC 7942 from Cyanobacteria**
Delia Teresa Sponza Cansu Doğanx
- 12 Effect of Ferroelectric Nanopowder on Electrical and Acoustical Properties of Cholesteric Liquid Crystal**
Santosh Mani Madhavi Pradhan Archana Sharma S..R.Chawade Sameer Hadkar
Krishnakant Mishra Jyoti Amare Pradip Sarawade

Copyright

Non-Metallic Material Science is licensed under a Creative Commons-Non-Commercial 4.0 International Copyright (CC BY- NC4.0). Readers shall have the right to copy and distribute articles in this journal in any form in any medium, and may also modify, convert or create on the basis of articles. In sharing and using articles in this journal, the user must indicate the author and source, and mark the changes made in articles. Copyright © BILINGUAL PUBLISHING CO. All Rights Reserved.



ARTICLE

Solving the Problem of Silicon Dioxide Melting Based on Deviation Model

Yuhan Sun^{1,2*} Na Huang^{1,3} Jie Yu^{1,3}

1. North China University of Technology Mathematical Modeling Innovation Lab, Tangshan, Hebei, 063210, China

2. School of Metallurgy and Energy, North China University of Technology, Tangshan, Hebei, 063210, China

3. School of Chemical Engineering, North China University of Technology, Tangshan, Hebei, 063210, China

ARTICLE INFO

Article history

Received: 15 January 2020

Accepted: 15 January 2020

Published Online: 30 April 2020

Keywords:

Image superposition

Deviation model

Interpolation test

ABSTRACT

In order to reveal the dissolution behavior of iron tailings in blast furnace slag, we studied the main component of silica in iron tailings. First, edge contour features need to be established to represent the melting process of silica. We choose shape, perimeter, area and generalized radius as objects. By independently analyzing the influence of these four indexes on the melting rate, the area and shape were selected as the characteristic parameters of the edge contour of the silica particles. Then, the actual melting rate of the silica is estimated by the edge contour feature index. Finally, we can calculate the melting rate of the first second of three time periods of 0.00010312mm³/s, 0.0002399mm³/s, 0.0000538mm³/s.

1. Introduction

Background

Silica has stable physical and chemical properties, it has a high melting point and boiling point, it doesn't react with acid. And hot strong alkali solution, molten caustic soda, reaction to silicate and water. At high temperature, it reacts with a variety of metal oxides, silicate formation. Therefore, in the tailings waste of various mines, silica often occurs. Let's take iron tailings as an example, in China, the content of silicon dioxide in some iron tailings can reach 75%. As a result of silica has high melting and boiling point, highest than others. Therefore, when people are smelting metal ore, so melting behavior of silica expresses melting behavior of iron tailings tank^[1]. But, the temperature of high temperature melting pool exceeds 1500 °C, when measuring the temperature of silica

in the high temperature melting pool by direct contact, will lead to shorter instrument life. Therefore, relevant research groups utilization system, which a CCD video shooting system with magnification effect. Analyzed the fixed value rate of silica in time series, tracked the process of silicon dioxide heating and melting.

In order to analyze the melting behavior of silicon dioxide better, the index which can describe the edge profile of silicon dioxide is established.

According to the characteristic index of silica edge profile, a three-dimensional model of silica particles is established. The volume of silicon dioxide particles is determined by the establishment of three-dimensional model, and the actual melting rate of silicon dioxide is determined by the reduction of the volume of silicon dioxide particles in the photos taken by the CCD video shooting system^[2].

*Corresponding Author:

Yuhan Sun,

North China University of Technology Mathematical Modeling Innovation Lab, Tangshan, Hebei, 063210, China; School of Metallurgy and Energy, North China University of Technology, Tangshan, Hebei, 063210, China;

Email: 1643360071@qq.com

2. Problem Analysis

According to the requirements of the topic, we need to set a series of indicators, to characterize the edge profile of silica. Find out the relationship, which the relationship between index and silicon dioxide melting process. Finding indicators, which index having decisive influence on the melting rate of silica. Physical properties of four kinds of silica particles, which shape, perimeter, area and generalized radius, to analyze the change of perimeter. By building lattice on time series graph, analysis of silica particles, which area and radius^[3]. Also, high temperature treatment to silica, analyzed the relationship, which shape and melting rate. Through the comparison of four indexes, determined the edge contour feature index.

From the fact that the known mass is proportional to the three-dimensional volume, the density of silica is a constant value. Therefore, we turn complexity into general. also, we have replaced silicon dioxide of unknown shape and size with exact shape. In the second question, number of small squares, it represents the area index with the largest correlation coefficient. Then, we divided the picture into three stages. Using SPSS regression, fitting method, drawn the function curve, which melting rate and area of silica. Lists the corresponding function expressions, to obtain the actual melting rate of silica.

3. Assumptions

(1) Assumed the air resistance is not considered during the movement of silica.

(2) Assumed the static friction with the crucible will not be taken into account when the silica particles move.

(3) Assumed that the viscous force produced by the relative motion of silica with air is not taken into account.

(4) Assumed that the polymerization between silicon dioxide and oxygen molecules is not considered.

(5) Assumed that when corundum crucible heats silicon dioxide, the heating temperature of silicon dioxide does not change.

4. Determination of Edge Contour Index

To determine indicators, which the profile of silica that can represent the melting process. We chose four indicators, that shape, perimeter, area and generalized radius. Research separately, that whether these indexes are related to melting rate^[4].

4.1 Shape

In the melting process, shape of silica, which from irreg-

ular shape to approximate cylinder, and then gradually approach to the sphere. For the sake of study, whether the melting process is related to shape, we can do experiments to verify it. In the experiment, we make the slag into a cylinder, as the temperature increases. Liquid volume will increase, sample shape will change, cylindrical specimen is sintered and shrinks. And then gradually melt, the height of the sample keeps decreasing^[5]. As shown in Figure 1.

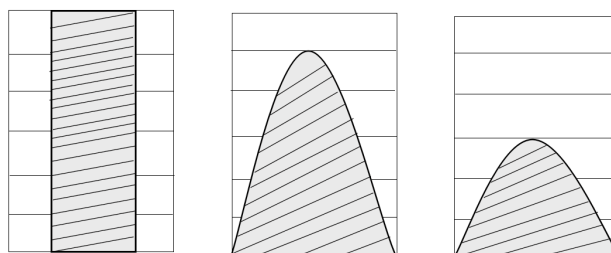


Figure 1. Specimen height change during melting

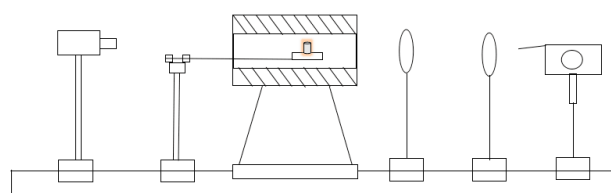


Figure 2. Melting point and melting temperature measuring device

As shape changes, like that, this experiment verifies the impact, which solid shape vs. melting rate. With the aid of the instrument shown in Figure 2, by adjusting the position of the objective and eyepiece, make the sample image on the screen, which clear magnified image. Then adjust the up and down positions on the left and right of the screen, place the magnified image of the sample, between the six horizontal scale lines of the screen. To observe the melting characteristic temperature. At a certain heating rate, continuously record the remaining area of melting. Then we can get the curve, which melting rate changes with time. It can be seen from the curve, that when the solid shape changes from cylinder to mound, increase of melting rate^[6]. Similarly known, in the melting process of silica, when the shape changes from irregular objects to regular objects, increase of melting rate.

4.2 Area

In the melting process of silica, from start to end, silicon dioxide area is decreasing. To explore the relationship, which between melting rate and area, we can calculate the area of silica in 1s. Then, put silicon dioxide melting diagram on grid line, use small grid to express area. As

shown in Figure 3.

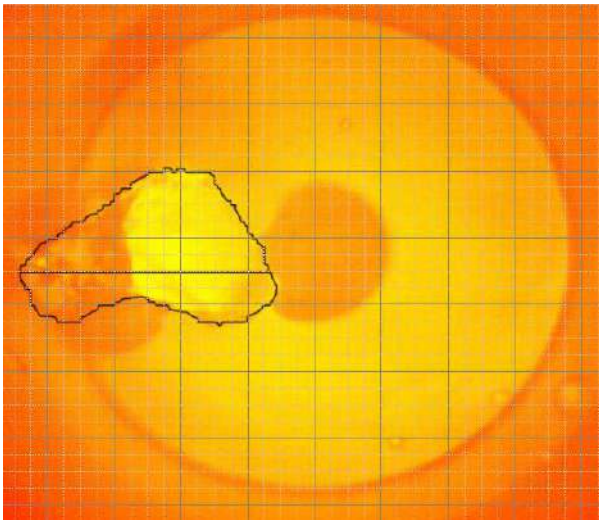


Figure 3. Calculation diagram of area, perimeter and generalized radius

Thus, we can calculate the residual area of silicon dioxide at each time. Select three melting stages, each segment of 10s. The first stage is the initial stage of melting, from 497 to 506. The second stage is the intermediate melting stage, from 550 to 559. The third stage is the final melting stage, from 592 to 601. As shown in Table 1 (Data from the following tables, is phase I and phase II. In the molten state, area, perimeter and diameter's data. See the appendix for the data of the third stage.) According to unit time, reduction of area. Can obtain the relationship between area and melting rate.

Table 1. Edge profile index data

| Stage one | Area | Perimeter | Diameter | Stage two | Area | Perimeter | Diameter |
|-----------|------|-----------|----------|-----------|------|-----------|----------|
| 497 | 130 | 49 | 16 | 550 | 38 | 34 | 10 |
| 498 | 123 | 53 | 18 | 551 | 28 | 26 | 8 |
| 499 | 113 | 54 | 17 | 552 | 26 | 25 | 7 |
| 500 | 111 | 53 | 19 | 553 | 23 | 18 | 6 |
| 501 | 109 | 43 | 13 | 554 | 19 | 23 | 7 |
| 502 | 95 | 45 | 14 | 555 | 20 | 22 | 7 |
| 503 | 81 | 40 | 15 | 556 | 22 | 22 | 7 |
| 504 | 78 | 38 | 14 | 557 | 18 | 20 | 8 |
| 505 | 74 | 42 | 10 | 558 | 16 | 17 | 6 |
| 506 | 60 | 48 | 12 | 559 | 14 | 14 | 5 |

The area reduction rate, of the three stages is shown in Figure 4. Can be found, melting rate of the third stage, significantly less than the first stage. Therefore, we can come to a conclusion, the smaller the area, less contact

with the outside world. So less heat absorption, the slower the cooling rate^[7].

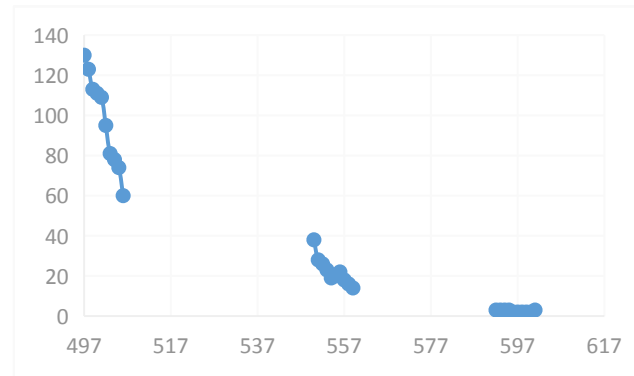


Figure 4. Area change with time

4.3 Perimeter

To explore the process of melting, relationship, that circumference and melting rate. We still choose three stages, to when exploring the area. Circle silica, the number of small lattices surrounding silica is the perimeter length. As shown in Figure 3. According to the change of perimeter in Table 1. We can come to a conclusion: Because of the uneven melting in some places, cause circumference not to change linearly. As shown in Figure 5. So the perimeter does not represent the melting process of silica.

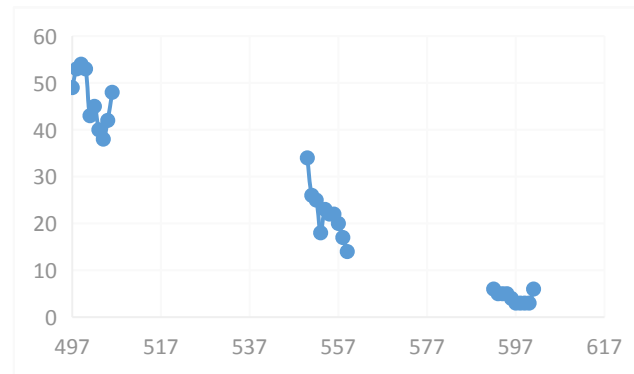


Figure 5. Variation of circumference with time

4.4 Generalized Radius

Redefining the melting state, the longest radius of silicon oxide is the generalized radius. Empathy, the above three stages are still selected, calculating the length of the generalized radius. To reduce the error, we chose the diameter and length here. As shown in Figure 3. And organize the data into table 1. From what we can get, according to figure 6, the relationship between generalized radius and time. So generalized radius can not represent process, which the melting process of silica.

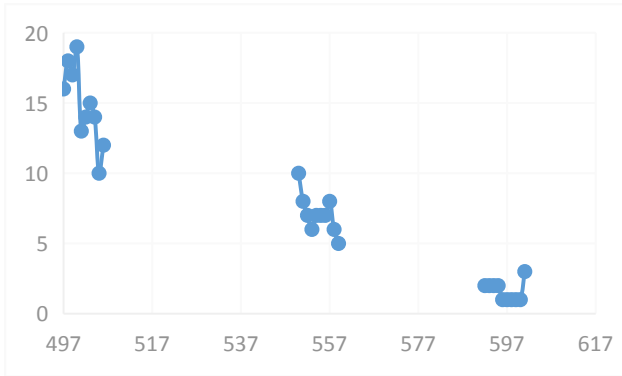


Figure 6. Generalized radius versus time

5. Deviation Model based on Melting Rate

5.1 Model Preparation

The mass is directly proportional to the 3D volume, indicating that the density of silicon dioxide is constant. It can be seen from the review that the density of silicon dioxide is 2.2 ~ 2.66g/cm³. Generally, in the heating process, the volume of drugs will not exceed 2/3 of the total volume, so the density of silicon dioxide can be taken as 2.4g/cm³, and the volume V=64mm³, so it can be seen from $m = \rho V$, $m = 0.1536g$, the mass m is 0.1536g. We know that the shape and area can represent the edge contour characteristics of the silicon dioxide melting process [8]. Because the shape of silicon dioxide will change randomly with the melting process, the shape is an unstable parameter. Therefore, we can choose regular prism as the initial solid in this topic.

5.2 Establishment and Solution of the Model

Taking the prismatic silicon dioxide crystal with mass of 0.1536g as an example, according to the influence of the area on the melting rate, SPSS can be used to fit the change of the area of three stages with time, that is, the melting rate of silicon dioxide in unit time. Because the key parameter of silicon dioxide melting rate is mass, and the melting rate is directly proportional to mass, if there is no influence of area on the melting rate, the corresponding relationship between them should be linear function. Now, the actual melting rate of silicon dioxide is estimated by the edge profile characteristic index of silicon dioxide.

Analyze the impact of the first phase, which influence of area on melting rate. Fitting with SPSS, get the function of area changing with time. Establish deviation model. It is found, that the fitting degree of cubic function is the highest $R^2=0.978$. As shown in Figure 7. According to the fitted coefficient, get the relationship between area and time: $x=0.198t^3-0.597t^2-0.589t$, this is the effect of area on

melting rate. Plus, the effect of mass on melting rate. So, the relationship between melting rate and these two factors is

$$V_1=am+b(0.198t^3-0.597t^2-0.589t)$$

$R^2=0.978$. Fair and reasonable, the second melting rate is

$$V_2=am+b(3.866t^3-7.133t^2-2.584t)$$

$R^2=0.681$. As shown in Figure 8. The third melting rate is

$$V_3=am+b(10.135t^3-14.170t^2+3.878t),$$

$$R^2=0.936. \text{ As shown in Figure 9.}$$

Therefore, in the three stages, the relationship between melting speed and time is as formula (1).

$$\begin{cases} V_1=am+b(0.198t^3-0.597t^2-0.589t), R^2 = 0.978 \\ V_2=am+b(3.866t^3-7.133t^2+2.584t), R^2 = 0.681 \\ V_3=am+b(10.135t^3-14.170t^2+3.878t), R^2 = 0.936 \end{cases} \quad (1)$$

This formula is actual melting rate of melting rate. When the mass is 0.1536g, three stages first second, which instantaneous melting rate.

Namely: 0.00010312mm³/s, 0.0002399mm³/s, 0.0000538mm³/s.

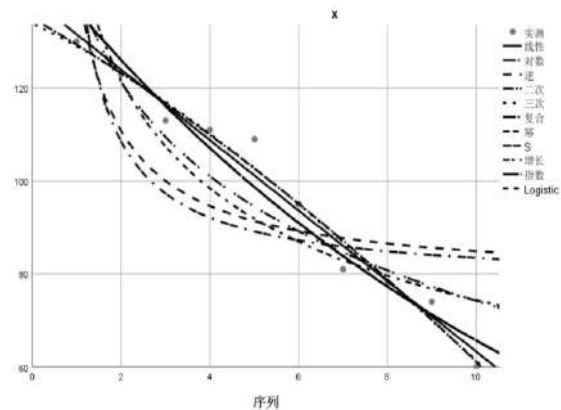


Figure 7. First stage fitting function diagram

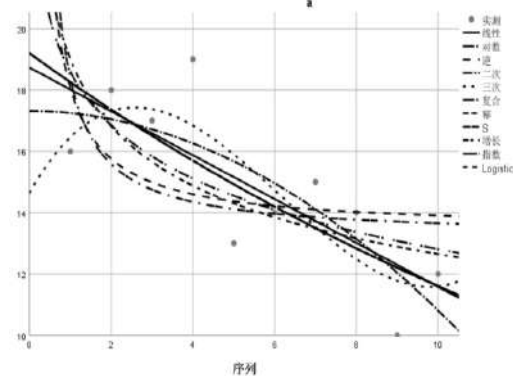


Figure 8. Second stage fitting function diagram

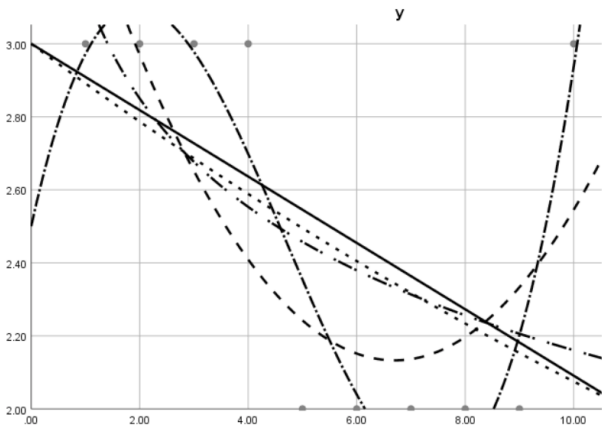


Figure 9. Third stage fitting function diagram

6. Conclusion

From the above analysis we can obtain the relationship between shape, area, perimeter and generalized radius and melting rate. The area has the greatest relationship with the melting rate. The smaller the area, the smaller the contact with the outside world, the smaller the heat absorption, and the slower the cooling rate. There is a certain correlation between the shape and the melting rate. During the melting process of silica, the melting rate increases when the shape changes from irregular object to regular object. However, the influence of shape on the melting rate is not as great as that of area. Perimeter and generalized radius have no or little correlation with melting rate and have no decisive influence on the change of melting rate. Therefore, area is selected as the characteristic parameter of the edge contour of silica particles, and the shape of silica particles is taken as a reference, while perimeter and generalized radius are not suitable for the characteristic parameters of the edge contour of silica particles.

We use the image overlay technology of MATLAB to process 114 pictures. Then 10 photos are selected from three stages for regression analysis, and the most characteristic index area of edge contour is used to solve the melting rate of silica. After SPSS regression fitting, the fitting curve of three stages can be drawn. When the mass is 0.1536g, the instantaneous melting rates in the first second of the three stages are 0.00010312mm³/s, 0.0002399mm³/s and 0.0000538mm³/s.

7. For Inspection of the Models

The actual melting rate of silica based on the best fitting degree selected by SPSS fitting, according to the fitting function $p(x) = a + bx^j$, three functions are fitted out, and that:

$$a = \left(\sum_{i=1}^m y_i \sum_{i=1}^m x_i^2 - \sum_{i=1}^m x_i \sum_{i=1}^m x_i y_i \right) \left(m \sum_{i=1}^m x_i^2 - \left(\sum_{i=1}^m x_i \right)^2 \right)$$

$$b = \left(m \sum_{i=1}^m x_i y_i - \sum_{i=1}^m x_i y_i \right) \left(m \sum_{i=1}^m x_i^2 - \left(\sum_{i=1}^m x_i \right)^2 \right)$$

$$R = \frac{\sum_{i=1}^m x_i y_i - \frac{1}{m} \sum_{i=1}^m x_i \sum_{i=1}^m y_i}{\sqrt{\left[\sum_{i=1}^m x_i^2 - \frac{1}{m} \left(\sum_{i=1}^m x_i \right)^2 \right] \left[\sum_{i=1}^m y_i^2 - \frac{1}{m} \left(\sum_{i=1}^m y_i \right)^2 \right]}}$$

In general, $R > 0.95$ can be considered to have a good correlation. According to the calculation of the third question, the R index obtained ($R_1=0.989$, $R_2=0.825$, $R_3=0.935$) can indicate that the first stage conforms to the fitting function. This is the actual melting rate of silica.

References

- [1] Hong Zeng, Jian He, Lin Wu, Songquan Zhang, Daiyin Zhao, Zhaohong Yang, Xiufang Gong, Gongxian Yang. Application of amorphous silica in investment casting[J]. Dongfang turbine, 2019(01): 55-57.
- [2] Jianping Xu, Zhaoxiong Zhang. Determination of total silicon, silicon dioxide and other impurities in industrial silicon by melting sample preparation-x-ray fluorescence spectrometry[J]. Physical and chemical examination (chemical volume), 2019, 55(02): 187-192.
- [3] Ningning Wang. Study on polylactic acid copolymerization and nano silica composite modification[D]. Henan University, 2012.
- [4] Jingzhi Zheng. Dispersion and properties of polypropylene / micro and nano silica composites[D]. Huazhong University of science and technology, 2010.
- [5] Wei Zhou. Study on the preparation of nano and micro silica particles by melting[D]. Wuhan University of technology, 2010.
- [6] Xi Liu. Preparation and properties of nylon 6 grafted on the surface of nano silica[D]. Hunan University, 2010.
- [7] Jing Qian, Ruixia Yang, Chao Li. Determination of silica in fluorspar[J]. Metallurgical standardization and quality, 2009, 47(03): 41-43.
- [8] Chen Minjie, Tian Guohua, Zhang Yong, Wan Chaoying, Zhang Yinxi. Effect of silica on crystallization and melting behavior of isotactic polypropylene and copolymerized polypropylene[J]. China plastics, 2005(10): 30-34.



ARTICLE

Effects of Polypyrrole / Graphene Oxide Composites with Different Reaction Times on Electrochemical Performance

Minzhen Feng Wei Lu* Ranran Zhen Ya Wang Yun Zhou

Chongqing Key Laboratory of inorganic Function Materials, College of Chemistry, Chongqing Normal University, Chongqing, 401331, China

ARTICLE INFO

Article history

Received: 10 February 2020

Accepted: 10 February 2020

Published Online: 30 April 2020

Keywords:

Graphene oxide

Polypyrrole

Supercapacitors

ABSTRACT

Graphene oxide (GO) was prepared using the modified Hummers method and used as a template for polypyrrole. Polypyrrole was polymerized in situ on the surface of GO to finally obtain the polypyrrole/graphene oxide composite material. The effects of different reaction times on the electrochemical performance of polypyrrole/graphene oxide in the second step were studied. It was obtained that the composite material had optimal properties when the reaction time was 24 h.

1. Introduction

With the development of today's society, people's demand for energy is increasing. The development and application of new energy are imminent. As a new type of energy storage device, supercapacitor has been widely used in various fields such as electric vehicles, communications, and industrial production. Because of its advantages such as fast charging speed and high power density, it has been widely used in various fields such as electric vehicles, communications, and industrial production^[1-3]. It is well known that supercapacitors correspond to different electrode materials according to different energy storage mechanisms^[4-6]. At present, common electrode materials include carbon nanotubes, biomass carbon and other high specific surface area carbon materials, metal oxides, and high-molecular

conductive polymers. Conductive polymers have attracted much attention because of their good electrical conductivity and higher specific capacitance. Among many conductive polymers, polypyrrole is considered to be one of the most valuable electrode materials due to its characteristics of cheap raw materials, simple synthesis, and high theoretical capacitance. However, due to its poor mechanical properties, the polypyrrole has a significant change in volume after multiple charge and discharge tests at high rates, and its conductivity decreases. As a result, the polypyrrole exhibits a poor capacitance retention rate and a rapidly decaying capacitance^[7-10].

In order to improve the shortage of pure polypyrrole, polypyrrole can be combined with carbon materials to improve its performance. Such as graphene oxide, biomass carbon, activated carbon and so on. Among many carbon

*Corresponding Author:

Wei Lu,

Chongqing Key Laboratory of inorganic Function Materials, College of Chemistry, Chongqing Normal University, Chongqing, 401331, China;

Email: mailluwei666@126.com

materials, graphene oxide has a wrinkled surface, which results in graphene oxide having a large specific surface area. In addition, the surface of graphene oxide has a large number of oxygen-containing functional groups, so that it has better water solubility, which is conducive to better dispersion of graphene oxide in water. In order to provide more active sites for polypyrrole, the polypyrrole nanospheres are embedded on the graphene oxide substrate. However, the reaction time for the synthesis of polypyrrole has a great impact on the morphology of polypyrrole and its performance in super capacitors. In this paper, modified Hummers method was used to prepare graphene oxide^[11]. Polypyrrole nanospheres were prepared on the surface of graphene oxide by in-situ polymerization. At the same time, the optimal reaction time of polypyrrole were discussed.

2. Experimental Part

2.1 Experimental Reagent

Hydrogen peroxide, Potassium hydroxide, Graphite, Sodium nitrite, Sulfuric acid, Potassium permanganate, Absolute ethanol, Chlorhydric acid, Pyrrole, Ammonium persulfate(APS), N-methylpyrrolidone, Acetylene black, Carbon paper. All medicines were purchased from research technology suppliers and used without further purification.

2.2 Experimental Process

(1) Synthesis of graphene oxide by improved Hummers method^[11]. 60 ml of dilute hydrochloric acid was mixed with 20 ml of ethanol solution, and 36 mg of graphene oxide solid powder was added thereto. The above mixed solution was dispersed uniformly by ultrasound, and then pyrrole monomer was added.

(2) Take a certain amount of APS and dissolve it in 20 ml of dilute hydrochloric acid to obtain the pre-prepared mixed solution.

The above two solutions were stirred in a water bath below 0°C. Slowly add the pre-prepared mixed solution to the liquid mixed with graphene oxide, and react the mixed solution in the ice bath for 6 h, 12 h, 18 h, and 24 h. Finally, the resulting solution was suction filtered and washed with dilute HCl, ethanol and deionized water in this order. Dry in a vacuum oven at 60°C for 10 h. The obtained product was a polypyrrole/graphene oxide composite (PPy/GO).

2.3 Test Equipment

Cyclic voltammetry and constant current charge and dis-

charge tests were performed on all samples using H₂SO₄ as electrolyte in Shanghai Chen Hua CHI660E. The cyclic voltammetry test voltage is -0.2~0.8 V, Ag/AgCl is the reference electrode, Pt sheet electrode is the counter electrode, and the test sample is the working electrode; Charge/discharge test voltage selection range is 0~0.8 V.

3. Results and Discussion

3.1 Electrochemical Testing of Materials

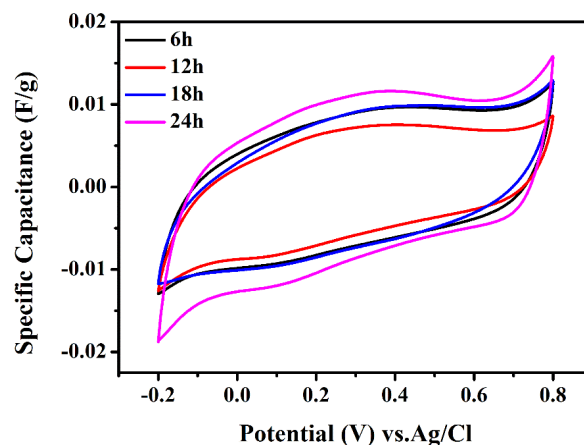


Figure 1. Cyclic voltammetry curves of PPy/GO with different reaction times

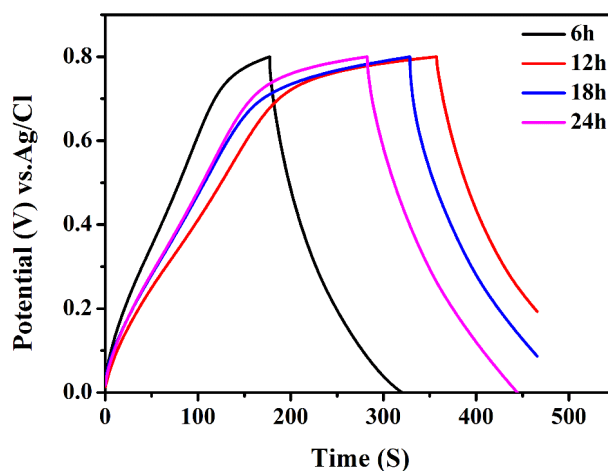


Figure 2. Charge/discharge of PPy/GO with different reaction times

Figure 1 is a cyclic voltammetry diagram of PPy/GO prepared at different reaction times. The scan rate is 20 mv s^{-1} , and the test voltage is -0.2 V to 0.8 V. It can be seen that the shapes of all the curves are almost the same. Protrusions appear on the scan curves. This is because during the test, the sample has undergone a redox reaction and exhibited a redox peak. It can also be seen from Fig-

ure 1 that when the reaction time is 24 h, the area enclosed by the CV curve is the largest. This shows that under this reaction time, the sample has a larger specific capacitance [12-13].

Figure 2 is a GCD chart of samples prepared at different reaction times. It can be seen from the figure that the performance of PPy/GO with a reaction time of 24 h is the best. Although the discharge time of PPy/GO with a reaction time of 24 h is lower than that of the 12 h and 18 h samples, the reaction discharge part of the former two is not fully discharged, which has a greater impact on the stability of the sample [14-15].

4. Conclusions

In short, graphene oxide prepared by the improved Hummers method has a large specific surface area. The effects of different reaction times on the electrochemical performance of PPy/GO composites were discussed. It was finally obtained that the PPy/GO composite had the best electrochemical performance when the reaction time was 24 h. In general, as the research continues, the optimization of PPy/GO will become more in-depth. I believe that PPy/GO will definitely become one of the most popular electrode materials in the future.

Acknowledgements

This work was supported by national natural science foundation of China (21504010); Open project of engineering research center of active material biotechnology, ministry of education, Chongqing normal university (AS201609).

References

- [1] Wang Y., Shi Z., Huang Y., et al. Supercapacitor Devices Based on Graphene Materials[J]. *Journal of Physical Chemistry*, 2009, 113(30): 13103-13107.
- [2] Frackowiak, Elzbieta. Carbon materials for supercapacitor application[J]. *Physical Chemistry Chemical Physics*, 2007, 9(15): 1774-0.
- [3] Snook G A , Kao P., Best A S.. Conducting-polymer-based supercapacitor devices and electrodes[J]. *Journal of Power Sources*, 2011, 196(1): 1-12.
- [4] Yang H , Kannappan S , Pandian A S , et al. Graphene supercapacitor with both high power and energy density[J]. *Nanotechnology*, 2017, 28(44): 445401.
- [5] He Y., Chen W., Li X., et al. Freestanding Three-Dimensional Graphene/MnO₂ Composite Networks As Ultra light and Flexible Supercapacitor Electrodes[J]. *ACS NANO*, 2013, 7(1): 174-182.
- [6] Borenstein A , Hanna O., Attias R., et al. Carbon-Based Composite Materials for Supercapacitor Electrodes: A Review[J]. *Journal of Materials Chemistry A*, 2017, 5(25).
- [7] Siuzdak K., Bogdanowicz R.. Nano-engineered diamond-based materials for supercapacitor electrodes: A review[J]. *Energy Technology*, 2017.
- [8] Carratalá-Abril J., Rey-Martínez L., Beneito-Ruiz R., et al. Development of Carbon-based Composite Materials for Energy Storage[J]. *Materials Today: Proceedings*, 2016, 3: S240-S245.
- [9] Liu Y., Nie C., Liu X., et al. Review on carbon-based composite materials for capacitive deionization[J]. *RSC Adv.* 2015, 5(20): 15205-15225.
- [10] Ke Q., Wang J.. Graphene-based Materials for Supercapacitor Electrodes - A Review[J]. *Journal of Materials*, 2016: S2352847816000022.
- [11] Hummers W S, Offeman R E. Preparation of Graphitic Oxide[J]. *Journal of the American Chemical Society*, 1958, 208: 1334-1339.
- [12] Zhang X., Ma L., Gan M., et al. Fabrication of 3D lawn-shaped N-doped porous carbon matrix/polyaniline nanocomposite as the electrode material for supercapacitors[J]. *Journal of power sources*, 2017, 340(FEB.1): 22-31.
- [13] Rasouli H., Naji L., Hosseini M G.. 3D structured polypyrrole/reduced graphene oxide (PPy/rGO)-based electrode ionic soft actuators with improved actuation performance[J]. *New Journal of Chemistry*, 2018, 42.
- [14] Liu W., Fang Y., Xu P , et al. Two-Step Electrochemical Synthesis of Polypyrrole/Reduced Graphene Oxide Composites as Efficient Pt-Free Counter Electrode for Plastic Dye-Sensitized Solar Cells[J]. *ACS Applied Materials & Interfaces*, 2014, 6(18):16249-16256.
- [15] Fan X., Yang Z., He N.. Hierarchical nanostructured polypyrrole/graphene composites as supercapacitor electrode[J]. *RSC Advances*, 2015, 5(20): 15096-15102.



ARTICLE

Bio-fuel Production From Carbondioxide Gas Using *S. elongatus* PCC 7942 from Cyanobacteria

Delia Teresa Sponza^{1*} Cansu Doğanx²

1. Environmental Engineering Department, Engineering Faculty, Dokuz Eylül University, Buca-İzmir, Turkey

2. Sciences Institute, Department of Biology, Science Faculty, xAgean University, Turkey

ARTICLE INFO

Article history

Received: 17 April 2020

Accepted: 26 April 2020

Published Online: 30 April 2020

Keywords:

Bio-Fuel

Carbondioxide GAS *S. elongatus*

Cyanobacteria

1-butanol

ABSTRACT

The aim of this study, is 1-butanol production using CO₂ with *S. elongatus* PCC 7942 culture. The yields of 1-butanol_{produced}/CO_{2utilized} have been calculated. The maximum concentration of produced 1- butanol is 35.37 mg/L and 1-butanol_{produced}/CO_{2utilized} efficiency is 92.4. The optimum operational conditions were 30°C temperature, 60 W intensity of light, pH= 7.1, 120 mV redox potential, 0.083 m³/sn flow rate with CO₂ and 0.5 mg/l dissolved O₂ concentration. Among the enzymes on the metabolic trail of the production of 1-butanol via using *S. elongatus* PCC 7942 cyanobacteria. At maximum yield; the measured concentrations are 0.016 µg/ml for hbd; 0.0022 µg/ml for Ter and 0.0048 µg/ml for AdhE2. The cost analyses necessary for 1-butanol production has been done and the cost of 1 liter 1-butanol has been determined as 1.31 TL/L.

1. Introduction

The carbon dioxide levels in the atmosphere elevated 2,2 – 3,2 ppm every year, since the fossils was combusted. Although carbon dioxide in air was in minor level (between 0,01–0.036 %) it's concentration elevated significantly in municipal metropoullitan areas and industrial regions. The carbon dioxide level in the air increase 2,2 – 3,2 ppm in every year due to utilisation of fossil fuels as heating. The carbon dioxide concentrations in the organized fabriks was measured as high as 600-700 ppm^[1]. 86 % of carbon dioxide in the air generated from the utilization of fuels (petroleum, coal and methane gas). 19 % of the carbon dioxide present in air coming from the humans, from the air pollutants and from the microorganisms by cleaving the complex organics. The contamination increase since petroleum, coal and methane

gas were continuously utilized. The experimental studies aim to decrease the carbon dioxide concentrations to the lower level (400 ppm) by decreasing the CO₂ emissions 60-85 % in year 2055. The green energy source 1-butanol is an candidate in the utilisation as fuel in the comparison to gasoline and methane. It can be produced by the wastes, it can be used as a source for heat, as car and motor fuel. By attaining the gasoline's place, 1-butanol is considered as an alternative to the potential fuel. The energy density of 1-butanol is 27 MJ/L. When compared, it has an energy density which is close to gasoline (32 MJ/L) and higher than ethanol (21 MJ/L)^[2]. Besides, the CO₂ emission from the gasoline used for vehicles and derivatives exhausts and this constitutes a great threat for global warming. As the carbon in 1-butanol is obtained from *S. elongatus* PCC 7942's segmenting the carbon dioxide in

*Corresponding Author:

Delia Teresa Sponza,

Environmental Engineering Department, Engineering Faculty, Dokuz Eylül University, Buca-İzmir, Turkey;

Email: delya.sponza@deu.edu.tr

the weather, burning 1-butanol does not cause a significant increase in carbon dioxide in the Earth's atmosphere. In the comparison of the costs of gasoline, the cost of 1-butanol is 3,8 times cheaper. Nowadays, the cost of 1 liter of gasoline is 4,98 TL/L. The maximum cost of 1 liter of 1-butanol was found to be 1,31 TL/L in this study. Therefore, 1-butanol, as an alternative source to gasoline will both reduce the cost and be used sustainably and widely as a renewable energy source.

Nitrogen, phosphorus and inorganic carbon it is important growth parameters for generation of *S. elongatus*. Inorganic carbon source CO₂ in the polluted industrial regions at high levels stimulates the growth of *S. elongatus* [8,9]. Atsumi et al., found that *S. elongatus* grow at very high rate in regions containing high CO₂ levels compared to clean district areas [3]. It was determined that elevated CO₂ levels improve the photosynthesis in these bacteria. As aforementioned *S. elongatus* PCC 7942 Cyanobacteria types decrease the carbon dioxide percentages in the polluted air and can be fixing easily from the oceans, lakes and rivers. 1-butanol is a primary alcohol with a four carbon structure and its chemical formula is C₄H₉OH. Its molecular weight 74.1216 g/mol, is colorless and have the same density as water. 1-Butanol can be accepted as a candidate energy source and can be used as energy instead of gasoline. The energy efficiency of 1-butanol (27 MJ/L) is higher than that of ethanol (21 MJ/L) and equivalent to that of gasoline (32 MJ/L) In addition, its hygroscopicity and compatibility also provide its excellent utilisation as energy source [2]. 1-butanol can be synthesized by butyryl-CoA from acetyl-CoA in Calvin cycle. 1-butanol production occurs by the existence of five enzymes: acetyl-CoA acetyltransferase (AtoB), 3-hydroxybutyryl-CoA dehydrogenase (Hbd), crotonase (Crt), trans-2-enoyl-CoA reductase (Ter) and aldehyde alcohol dehydrogenase (AdhE2) [3]. Recent studies showed that Cyanobacteria produce isobutyraldehyde, isobutanol [3], ethanol [4,5], ethylene [6], isoprene [7], sugars [8], and lactic acid [9]. The extensive synthesis of isobutanol and isobutyraldehyde from CO₂ indicates the feasibility of 1-butanol. Furthermore, CO₂ emissions which were the main pollutant source in the industrialized districts and in the villages can be converted to a helpful tool [1,2,3].

1-butanol which is used as biofuel will be the alternative to the gasoline in next days in the world. Compared to gasoline, 1-butanol is more economical and eco-friendly [10,11,12]. *S. elongatus* PCC 7942 is obtained by splitting the CO₂ in the air so the carbon burned in 1-butanol doesn't cause an increase in earth's atmosphere [10,11]. With this reason, in order to prevent the increase of CO₂ in the atmosphere, the utilization of 1-butanol will be a strong

alternative for energy source in the future [10,12]. The cyanobacteria genus were extensively used in biofuel and energy productions due to its non-expensive cost, and the easily fixing reasons from the oceans, lakes, sediments, river and sea-sides [12,13]. They convert the CO₂ to 1-butanol using their photosynthetic properties.

1-butanol production from CO₂ with *S. elongatus* PCC 7942 culture was performed, in this study. The yields of 1-butanol_{produced}/CO_{2utilized} and the 1-butanol concentrations have been calculated.

2. Materials and Methods

The studies were carried with the optimum parameters which are 30°C temperature, 60W light intensity, pH = 7.1, 120 mV redox potential, 0,083 m³/sec debit together with 0,5 mg/l CO₂ and dissolved O₂ concentration. The *S. elongatus* PCC 7942 cultures used in the test were pure (ATCC 33912) and were isolated from the coasts of Foça Sea, a district of Izmir, a spring in the estate of Foça Balaban Mountain, estate of Reis Dere in Tahtalı Baraj Lake (reservoir), in Izmir-Turkey. The *S. elongatus* PCC 7942 was grown in BB-11 broth at 37°C which has an OD₇₃₀ level of 3.9–4.2 at 610 nm wave length in a Spectrophotometer [2,3]. In each study, the concentrations of 3-hydroxybutyryl-CoA dehydrogenase (hbd), trans-2-enoyl-CoA reductase (Ter) and bifunctional aldehyde alcohol dehydrogenase (AdhE2) enzymes were measured in an Agilent HPLC with an C-18 column. 1-Butanol and CO₂ emissions in the samples was measured in an Agilent GC-MS 7890-A system with flame ionization detector and DB-FFAP capillary column. The column flow was 3 ml/min and the retention time of 1-butanol was 2.485 min.

3. Results

The studies were carried with the parameters which are 30°C temperature, 60W light intensity, pH = 7.1, 120 mV redox potential, 0,083 m³/sec debit together with 0,5 mg/l CO₂ and dissolved O₂ concentration. The *S. elongatus* PCC 7942 cultures used in the test were pure (ATCC 33912) and were isolated from the coasts of Foça Sea, a district of Izmir, a spring in the estate of Foça Balaban Mountain, estate of Reis Dere in Tahtalı Baraj Lake (reservoir), in Izmir. In each study, the concentrations of 3-hydroxybutyryl-CoA dehydrogenase (hbd), trans-2-enoyl-CoA reductase (Ter) and bifunctional aldehyde alcohol dehydrogenase (AdhE2) enzymes which are among the ones exist on the metabolic pathway, were measured in spectrophotometer.

The maximum concentration of produced 1-butanol

is 35.37 mg/L and 1-butanol_{produced}/CO_{2utilized} efficiency is 92.4%. The maximum yields have been achieved under the optimum operation parameters which are 30°C temperature, 60 W intensity of light, pH= 7.1, 120 mV redox potential, 0.083 m³/sn flow rate with CO₂ and 0.5 mg/l dissolved O₂ concentration. Among the enzymes on the metabolic trail of the production of 1-butanol via using *S. elongatus* PCC 7942 cyanobacteria. At maximum yield; the measured enzyme concentrations were 0.016 µg/ml for hbd; 0.0022 µg/ml for Ter and 0.0048 µg/ml for AdhE2, respectively. The cost analyses necessary for 1-butanol production has been done and the cost of 1 liter 1-butanol has been determined as 1.31 TL/L.

In Calvin Chain 3-phosphoglycerate production provided by the rubisco enzym which i precursor in the binding of CO₂ to ribuloz-1,5 biphosphate. Ribuloz-1,5 biphosphate reduce the acetil-CoA to CoA'yaand as result 1-butanol was produced(Lan and Liao, 2012). In our study it was found that 1- butanol is produced via hbd enzym. This enzym oconvert the acetoacetyl-CoA to-hidroksibutiril-CoA resulting in 1- butanol production as the final product^[10,11].

4. Conclusions

Due to limited energy sources in Turkey the lowering of conventional energy souces like coal, fuel, and termic and some problems in the recovery of the energy sources necessitates the extensive utilization of the wind and sun energies as clean-green technologies. THerefore in this study we suggest the utilization of 1- butanol in the cars as alternative to gasoline. This will decrease the cost and it will be used as an new recyclable energy source.

Acknowledgement

This study was prepared in the scope of Master of Sciences in Biotechnology, and at the same time it was supported by the Department of Scientific Resource Project (2014.KB.FEN.035), in Dokuz Eylül University Graduate School of Natural and Applied Sciences. Also, the author acknowledged The Scientific and Technological Research council of Turkey (TÜBİTAK) for financial support (1002 - Quick Support Program).

References

- [1] Denhez, F.. Global Worming Chapter. İstanbul; Turkey NTV publication in Turkish, 2007.
- [2] Lan, E.I., Liao, J.C.. Metabolic engineering of cyanobacteria for 1-butanol production from carbon dioxide. *Metabolic Engineering*, 2011, 13: 353-363.
- [3] Atsumi, S. Hanai, T., Liao, J.C.. Non-fermentative

pathways for synthesis of branched-chain higher alcohols as biofuels. *Nature*, 2008, 451: 86–89.

- [4] Deng, M.D., Coleman, J.R.. Ethanol synthesis by genetic engineering in cyanobacteria'. *Applied and Environmental Microbiology*, 1999, 65: 523–528.
- [5] Dexter, J., Fu, P.C.. Metabolic engineering of cyanobacteria for ethanol production', *Energy & Environmental Science*, 2009, 2: 857–864.
- [6] Takahama, K. Matsuoka, M. Nagahama, K., Ogawa, T.. Construction and analysis of a recombinant cyanobacterium expressing a chromosomally inserted gene for an ethylene-forming enzyme at the psbAI locus. *Journal of Bioscience and Bioengineering*, 2003, 95: 302–305.
- [7] Lindberg, P. Park, S., Melis, A. Engineering a platform for photosynthetic isoprene production in cyanobacteria, using *Synechocystis* the model organism. *Metabolic Engineering*, 2010, 12: 70–79.
- [8] Niederholtmeyer, H. Wolfstadter, B.T. Savage, D.F. Silver, P.A., Way, J.C.. Engineering cyanobacteria to synthesize and export hydrophilic products. *Applied and Environmental Microbiology*, 2010, 76: 3462–3466.
- [9] Shen, C.R. Lan, E.I. Dekishima, Y. Baez, A. Cho, K.M., Liao, J.C.. Driving forces enable high-titer anaerobic 1-butanol synthesis in *Escherichia coli*', *Applied Environmental Microbiology*, 2011, 77: 2905–2915.
- [10] Boynton, Z.L. Bennet, G.N., Rudolph, F.B.. Cloning, sequencing, and expression of clustered genes encoding beta-hydroxybutyryl-coenzyme A (CoA) dehydrogenase, crotonase, and butyryl-CoA dehydrogenase from *Clostridium acetobutylicum* ATCC 824. *Journal of Bacteriology*, 1996, 178(11): 3015-3024.
- [11] Allakhverdiev, S.I. Nishiyama, Y., Suzuki, I., Tasaka, Y. Ana e Murata, N.. Genetic engineering of the unsaturation of fatty acids in membrane lipids alters the tolerance of *Synechocystis* to salt stress. *Proceedings of the National Academy of Sciences, Paris, France*.
- [12] Allakhverdiev, S.I. Sakamoto, A. Nishiyama, Y., Murata, N.. Inactivation of photosystems I and II in response to osmotic stress in *Synechococcus*: contribution of water channels', *Plant Physiology*, 2000, 122: 1201–1208.
- [13] Kuan, D. Duff, S. Posarac, D., Bi, X. Growth optimization of *Synechococcus elongatus* PCC 7942 in lab flasks and 2-D photobioreactor. *The Canadian Journal of Chemical Engineering*, 2015, 93: 640-647.
- [14] Murray, R., Badger, ve T. ve Andrews, J.. Photosynthesis and inorganic carbon usage by the marine cyanobacterium. *Synechococcus* sp. *Plant Physiology*, 1982, 70(2): 517-523.

**ARTICLE**

Effect of Ferroelectric Nanopowder on Electrical and Acoustical Properties of Cholesteric Liquid Crystal

Santosh Mani^{1,2*} Madhavi Pradhan² Archana Sharma¹ S..R.Chawade¹ Sameer Hadkar²
 Krishnakant Mishra² Jyoti Amare² Pradip Sarawade²

1. K. J. Somaiya College of Engineering, Vidyavihar (E), Mumbai, 400077, India

2. Department of Physics, University of Mumbai, Santacruz (E), Mumbai, 400098, India

ARTICLE INFO*Article history*

Received: 21 April 2020

Accepted: 26 April 2020

Published Online: 30 April 2020

Keywords:

Ferroelectric nanopowder

Cholesteric liquid crystal

Dielectric

Acoustical

Ultrasonic

ABSTRACT

The composite materials based on nanopowder dispersed liquid crystals are important both from fundamental research and device applications due to their unique properties such as improvement in various properties like electrical, optical, thermal, energy storage and spontaneous polarization etc. The proper selection of nanoparticle and its size which to be dispersed in particular liquid crystals is very important for a particular application. In the present study, a ferroelectric nanopowder of Barium Titanate (BaTiO₃) was dispersed in cholesteric liquid crystal and the same was confirmed by Fourier Transform Infrared (FTIR) Spectroscopy. The various acoustical properties like ultrasonic velocity, density, Adiabatic Compressibility, Rao Constant, Wada Constant and Acoustic Impedance were investigated by ultrasonic interferometer at room temperature at fixed frequency. The dielectric constant was determined by Precision Impedance Analyzer. In addition to these investigations, particle size and surface area were also measured. Our investigation shows enhanced in dielectric and acoustical properties which may be useful for device applications extensively in microelectronics, low cost- photovoltaic devices, and custom-shaped containers possibly applied as a coating..

1. Introduction

Liquid Crystals (LCs) are soft condensed matters which can flow like conventional liquids and also have properties of crystalline solids. They play vital role in modern technology due to their photonics and display applications like optical imaging, organic light emitting diodes, erasable optical disks, light modulators, full color electronic slides for computer aided design, optical antenna etc. ^[1-4]. However, drawbacks such

as limited temperature range, slow response to external stimuli and degradation over longer periods prevent LCs from utilization to their full potential, for various applications. In order to overcome or minimize these drawbacks, different approaches were explored by scientific community based on technological applications. Out of all these approaches, it was found that when a nanomaterial is dispersed in LC, there are no significant structural distortions as these materials combine order and mobility at nanoscale scale and hence appear as a perfect candi-

**Corresponding Author:*

Santosh Mani,

K. J. Somaiya College of Engineering, Vidyavihar (E), Mumbai, 400077, India;

Department of Physics, University of Mumbai, Santacruz (E), Mumbai, 400098, India;

Email: santoshmani@somaiya.edu; samphy2013@gmail.com

date for functional composites^[5-13].

The investigation performed by scientific community confirms that the dispersion of nanoparticle into LC has improved properties like polarization, response time, operating voltage and conductivity. The composite material also exhibits property of strong surface plasmon resonance due to the collective oscillation of conduction electrons. Therefore, dispersion of nanoparticles in liquid crystals can give rise to the tuning various properties^[14-19].

The advantage of dispersing ferroelectric nanoparticle over other nanoparticle is that they show more alignment in the direction of LC molecules for better electrical, optical, acoustical response. In addition with this, the anisotropic nature of these nanoparticle make them suitable candidate for variety of applications. The idea of dispersing ferroelectric nano-particles to LC emerges by the work by de-Gennes and Brochard. They found that the sensitivity to a magnetic field could theoretically be increased by adding ferromagnetic nanoparticles to nematic liquid crystals^[20-24]. The ferroelectric particles have a strong permanent dipole which will align the LC molecules locally with the particles which will be transmitted to the rest of the bulk via weak inter-particle. Various researchers have reported enhancement in optical, structural and thermal properties of liquid crystal after dispersing nanoparticles, however the effect of ferroelectric nanopowder on cholesteric LC is rarely reported^[9,10,19-31].

In the present study we have dispersed ferroelectric nanopowder of Barium Titanate (BaTiO_3) in cholesteric liquid crystals and its electrical and acoustical properties were investigated. We have also examined particle size and surface area of pure and nono-particle dispersed LC. The materials used in this work were procured from Sigma Aldrich and no further purification was performed. The ferroelectric nanopowder of Barium Titanate (BaTiO_3) was dispersed in cholesteric liquid crystal by ultrasonication a technique which is reported earlier^[32].

2. Results and Discussion

2.1 Dielectric Measurements

Dielectric properties of pure LC and composite material were studied in terms of frequency using Precision Impedance Analyser (Wayne Kerr 6500B,) by applying AC voltage at constant amplitude^[35]. The variation of dielectric constant with frequency for pure and nanopowder dispersed LC is shown in Figure 1.

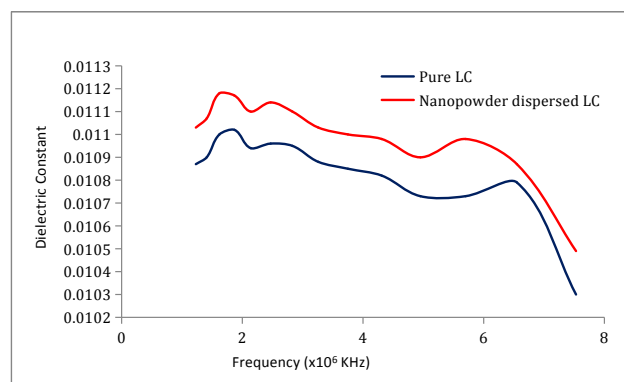


Figure 1. Variation of Dielectric Constant with frequency for pure and nanopowder dispersed LC

The dielectric constant increases when nanopowder of BaTiO_3 is dispersed in LC, which indicates in increase in electric flux density and conductivity. The dielectric constant increases due to the increase of space polarization. The enables the composite material to hold large quantity of electric charge for longer period of time and as also increases the capacity to store energy.

2.2 Determination of Specific Surface Area and Particle Size

The specific surface area and particle size were measured by BET Nitrogen adsorption. The specific surface area gives information about porosity, pore size distribution, shape, size, and roughness of the material under investigation. The specific surface area of pure LC was found $0.685 \text{ m}^2/\text{gm}$ whereas for manpowder dispersed LC it was found as $0.725 \text{ m}^2/\text{gm}$. The particle size plays an important role in various physical properties such as viscosity, heat and mechanical behavior and provides information about dispersion, solubility, nucleating efficiency, and optical properties of materials. The particle size of pure LC was found as 9.73 micron whereas for manpowder dispersed LC it was found 6.13 micron. The particle size reduction may be due to increasing the exposure of weak soluble by increasing surface area which improves the dissolution rate.

2.3 Measurement of Acoustical Parameter

These investigations were performed by Ultrasonic Interferometer (Mittal Enterprises) at room temperature with accuracy $\pm 0.1 \text{ ms}^{-1}$. For these investigations, ultrasonic wave of frequency 2MHz are generated by quartz crystal and allowed to reflect by another metallic plate which is kept parallel to it. The separation between these two plates is adjusted such that it is integral multiple of the waves formed in the medium which gives acoustic resonance.

Due to this, the current of anode becomes maximum and readings were recorded ^[7,23-24,31-33]. The various acoustic parameters were investigated which are shown in Table-2.

Table 2. The Different Acoustic Parameters for Pure and nanopowder dispersed LC

| Sample | Density ρ (gm/ml) | Velocity (m/s) | Adiabatic Compressibility β | Rao Constant (R) | Wada Constant (W) | Acoustic Impedance (Z) |
|-------------------------|------------------------|----------------|-----------------------------------|------------------|-------------------|------------------------|
| Toluene | 0.87 | 1310 | 6.62×10^{-10} | 1.14 | 2.18 | 1.14×10^6 |
| Pure LC | 0.91 | 1260 | 6.49×10^{-10} | 5.85 | 11.7 | 1.22×10^6 |
| Nanopowder Dispersed LC | 2.14 | 1280 | 2.85×10^{-10} | 1.18 | 2.18 | 2.74×10^6 |

The Rao Constant and Wada constant changes due to increase in velocity of nanopowder dispersed LC sample. The increasing in acoustical parameters suggests the increase in molecular density. The decrease in Adiabatic Compressibility indicates enhancement in degree of association among a liquid crystal and the significant structural after dispersing ferroelectric nanopowder in cholesteric liquid crystal. The increase in Acoustic Impedance suggests that molecular interactions after dispersing ferroelectric nanopowder in cholesteric liquid crystal are associative in the nature ^[34].

2.4 Fourier Transform Infrared Spectroscopy

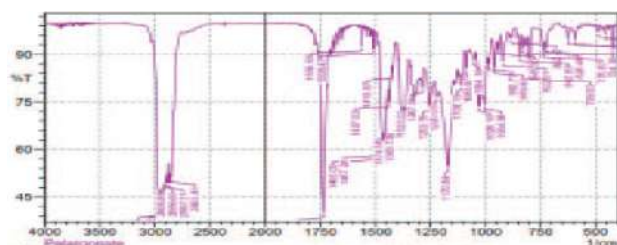


Figure 2. FTIR Spectrum of Pure LC

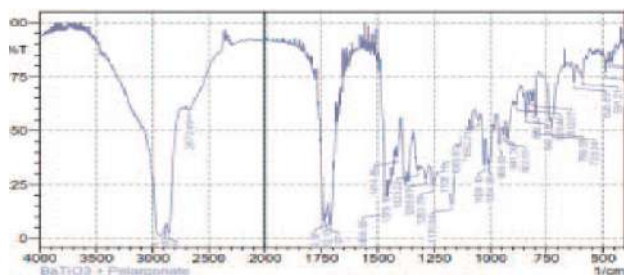


Figure 3. FTIR Spectrum of nanopowder dispersed LC

FTIR study indicates that the absorptions intensities in doped liquid crystals are reduced due to strong interaction of nanopowder with LC particles and new peaks emerging at 1400cm^{-1} - COO group, 3000cm^{-1} - 3100cm^{-1} indicat-

ing C-H stretching 3478cm^{-1} indicating C=O stretching due to strong presence of BaTiO_3 . Thus confirms the formation of nano composites of LC with BaTiO_3 .

3. Conclusions

(1) The effect of dispersing ferroelectric nanopowder of BaTiO_3 into cholesteric LC has been studied using acoustical and electrical measurements. The sensitivity of LC is enhanced after dispersing ferroelectric nanopowder which increases the performance of the LC.

(2) We observed that the ultrasonic velocities are lower in pure LC solution and increases after dispersing ferroelectric nanopowder which confirm greater association of molecules.. Ultrasonic velocity and hence adiabatic compressibility are structure depended properties which in turn are related to interlayer compelling and molecular orientation in the layer.

(3) This indicates that nanopowder dispersed LC are very useful in futuristic applications like device applications extensively in microelectronics, low cost- photovoltaic devices, and custom-shaped containers possibly applied as a coating.

References

- [1] P. J. Collings, Liquid Crystals: Nature's Delicate Phase of Matter, Princeton University Press, Princeton, 1990.
- [2] P. G. De Gennes, J. Prost. The Physics of Liquid Crystals 2nd Edn.. Oxford University Press, Oxford, 1995.
- [3] S. Chandrasekhar. Liquid Crystals 2nd Edn.. Cambridge University Press, Cambridge, 1992.
- [4] Krishnakant G. Mishra, S.K. Dubey, Santosh A. Mani, Madhavi S. Pradhan. Comparative study of nanoparticles doped in Liquid Crystal Polymer System. Journal of Molecular Liquids, 2016, 224: 668-671. <http://dx.doi.org/10.1016/j.molliq.2016.10.075>
- [5] Shri Singh. Impact of Dispersion of Nanoscale Particles on the Properties of Nematic Liquid Crystals. Crystals, 2019, 9: 475. <https://doi.org/10.3390/cryst9090475>
- [6] D. Demus, J. Goodby, G. W. Gray, H. W. Handbook of Liquid Crystals. Spiess and V. Vill, eds., Wiley-VCH, Weinheim, 1998, 1: 1-16.
- [7] V.K.Syal G.Lal P. Bisht S.Chauhan. Ultrasonic measurements of some 1:1 electrolytes in chlorobenzene + methanol mixtures. Journal of Molecular Liquids, 1995, 63(3): 317-328, [https://doi.org/10.1016/0167-7322\(94\)00795-X](https://doi.org/10.1016/0167-7322(94)00795-X)
- [8] CW Oh, EG Park, HG Park. Enhanced electro-optical properties in titanium silicon oxide nanoparti-

- cle doped nematic liquid crystal system *Surface and Coatings Technology*, 2019, 360(25): 50-55 , <https://doi.org/10.1016/j.surfcoat.2019.01.014>
- [9] S. Kaur, S. P. Singh, A. M. Biradar, A. Choudhary, K. Sreenivas. Enhanced electro-optical properties in gold nanoparticles doped ferroelectric liquid crystals. *Applied Physics Letters*, 2007, 91: 2, Article ID 023120.
- [10] Chinky, Pankaj Kumar, Vandna Sharma, Praveen Malik, K.K. Raina. Nano particles induced vertical alignment of liquid crystal for display devices with augmented morphological and electro-optical characteristics. *Journal of Molecular Structure*, 2019, 1196: 866-873, <https://doi.org/10.1016/j.molstruc.2019.06.045>
- [11] Praveen Malik, Ashok Chaudhary Rohit Mehra, K. K. Raina. *Electrooptic and Dielectric Studies in Cadmium Sulphide Nanorods/Ferroelectric Liquid Crystal Mixtures Advances in Condensed Matter Physics*. Hindawi Publishing Corporation, 2012: 8. Article ID 853160. DOI: 10.1155/2012/853160
- [12] A. Kumar, A. M. Biradar. Effect of cadmium telluride quantum dots on the dielectric and electro-optical properties of ferroelectric liquid crystals. *Physical Review E*, 2011, 83(4): 8. Article ID 041708.
- [13] Santosh A. Mani, Jyoti R. Amare, Sameer U. Hadkar, Krishnakant G. Mishra, Madhavi S. Pradhan, Hind Al-Johani & Pradip B. Sarawade. Investigations of optical and thermal response of polymer dispersed binary liquid crystals, *Molecular Crystals and Liquid Crystals*, 2017, 646(1): 183-193. <https://doi.org/10.1080/15421406>
- [14] Y. Shiraishi, N. Toshima, K. Maeda, H. Yoshikawa, J. Xu, S. Kobayashi. Frequency modulation response of a liquidcrystal electro-optic device doped with nanoparticles, *Applied Physics Letters*, 2002, 81(15): 2845-2847.
- [15] Y. Reznikov, O. Buchnev, O. Tereshchenko, V. Reshetnyak, A. Glushchenko, J. West. Ferroelectric nematic suspension, *Applied Physics Letters*, 2003, 82(12): 1917-1919.
- [16] C. I. Cheon, L. Li, A. Glushchenko et al. Electro-optics of liquid crystals doped with ferroelectric nano-powder. *SID International Symposium Digest of Technical Papers*, 2005, 36: 1471-1473.
- [17] F. Haraguchi, K. I. Inoue, N. Toshima, S. Kobayashi, K. Takatoh. Reduction of the threshold voltages of nematic liquid crystal electrooptical devices by doping inorganic nanoparticles. *Japanese Journal of Applied Physics* 2, 2007, 46(33-35): L796-L797.
- [18] Prakash, A. Choudhary, A. Kumar, D. S. Mehta, A. M. Biradar. Nonvolatile memory effect based on gold nanoparticles doped ferroelectric liquid crystal. *Applied Physics Letters*, 2008, 93(11). Article ID 112904.
- [19] A. Kumar, J. Prakash, D. S. Mehta, W. Haase, A. M. Biradar. Enhanced photoluminescence in gold nanoparticles doped ferroelectric liquid crystals. *Applied Physics Letters*, 2009, 95(2). Article ID 023117.
- [20] Krishnakant G. Mishra, S.K. Dubey, Santosh A. Mani, Madhavi S. Pradhan. Comparative study of nanoparticles doped in Liquid Crystal Polymer System. *Journal of Molecular Liquids*, 2016, 224: 668-671. <http://dx.doi.org/10.1016/j.molliq.2016.10.075>
- [21] X. Tong, Y. Zhao. Liquid-crystal gel-dispersed quantum dots: reversible modulation of photoluminescence intensity using an electric field. *Journal of the American Chemical Society*, 2007, 129(20): 6372-6373.
- [22] S.W. Lee, C.Mao, C. E. Flynn, A.M. Belcher. Ordering of quantum dots, using genetically engineered viruses. *Science*, 2002, 296(5569): 892-895.
- [23] V.K.Sayal, S. Chauhan, R. Gautam. Ultrasonic velocity measurements of carbohydrates in binary mixtures of DMSO + H₂O at 25°C. *Ultrasonics*, 1998, 36: 619-623, [https://doi.org/10.1016/S0041-624X\(97\)00104-2](https://doi.org/10.1016/S0041-624X(97)00104-2)
- [24] John P. Idoux, Cynthia K. McCurry, Tejraj M. Aminabhavi. Densities, Viscosities, Speeds of Sound, and Water Solubilities of Some Polypropylene Glycol Ether Derivatives in the Temperature Range. 273.15-323.15 K, *J. Chem. Eng. Data* 1994, 39(2): 261-265, <https://doi.org/10.1021/je00014a015>
- [25] A. S. Pandey, R. Dhar, S. Kumar, R. Dabrowski. Enhancement of the display parameters of 4_-pentyl-4-cyanobiphenyl due to the dispersion of functionalized gold nano particles. *Liquid Crystals*, 2011, 38(1): 115-120.
- [26] F. V. Podgornov, A. M. Suvorova, A. V. Lapanik, W. Haase. Electrooptic and dielectric properties of ferroelectric liquid crystal/single walled carbon nanotubes dispersions confined in thin cells. *Chemical Physics Letters*, 2009, 479(4-6): 206-210.
- [27] A. Chaudhary, P. Malik, R. Mehra, K. K. Raina, Electrooptic and dielectric studies of silica doped ferroelectric liquid crystal in SmC* phase, *Phase Transitions*, 2012, 85: 244- 254.
- [28] P. Malik, A. Chaudhary, R. Mehra, K. K. Raina. Electrooptic, thermo-optic and dielectric response of multiwalled carbon nanotube doped ferroelectric liquid crystal thin films. *Journal of Molecular Liquids*, 2012, 165: 7-11.
- [29] A. Kumar, J. Prakash, M. T. Khan, S. K. Dhawan,

- A. M. Biradar. Memory effect in cadmium telluride quantum dots doped ferroelectric liquid crystals. *Applied Physics Letters*, 2010, 97(16): 3. Article ID 163113.
- [30] P.Malik, A. Chaudhary, R. Mehra, K. K. Raina. Dielectric studies and memory effect in nanoparticle doped ferroelectric liquid crystal films. *Molecular Crystals and Liquid Crystals*, 2011, 541: 243-251.
- [31] Manisha G Bhave, Rita Gharde, Radha S. Comparative study of acoustic relaxation time of cholesteric liquid crystal and mixtures. 2016 IOP Conf. Ser.: Mater. Sci. Eng. 149 012202
DOI: 10.1088/1757-899X/149/1/012202
- [32] Rita A. Gharde, Madhavi S. Pradhan, Santosh A. Mani, Jyoti R. Amare. Electro-Optical Studies on Nanopowder Doped Liquid Crystal. *International Journal of Chemical and Physical Sciences, NCRTSM*, 2014, 3(Special Issue). ISSN: 2319-6602
- [33] Rita A. Gharde, Manisha G. Bhave. Ultrasonic Behaviour of Cholesteric Liquid Crystal. *IJ IJRSET*, 2015, 4(6).
DOI: 10.15680/IJRSET.2015.0406077
- [34] R.Mehra, Brij B. Malav. Ultrasonic, volumetric and viscometric studies of lactose in mixed solvent of DMF-H₂O at 298, 308 and 318 K. *Arabian Journal of Chemistry*, 2017, 10: S1894-S1900.
<https://doi.org/10.1016/j.arabjc.2013.07.018>
- [35] Rajendra R. Deshmukh & Anuja Katariya Jain. The complete morphological, electro-optical and dielectric study of dichroic dye-doped polymer-dispersed liquid crystal. *Liquid Crystals*, 2014, 41(7): 960+975.
<https://doi.org/10.1080/02678292.2014.896051>

Author Guidelines

This document provides some guidelines to authors for submission in order to work towards a seamless submission process. While complete adherence to the following guidelines is not enforced, authors should note that following through with the guidelines will be helpful in expediting the copyediting and proofreading processes, and allow for improved readability during the review process.

I . Format

- Program: Microsoft Word (preferred)
- Font: Times New Roman
- Size: 12
- Style: Normal
- Paragraph: Justified
- Required Documents

II . Cover Letter

All articles should include a cover letter as a separate document.

The cover letter should include:

- Names and affiliation of author(s)

The corresponding author should be identified.

Eg. Department, University, Province/City/State, Postal Code, Country

- A brief description of the novelty and importance of the findings detailed in the paper

Declaration

v Conflict of Interest

Examples of conflicts of interest include (but are not limited to):

- Research grants
- Honoria
- Employment or consultation
- Project sponsors
- Author's position on advisory boards or board of directors/management relationships
- Multiple affiliation
- Other financial relationships/support
- Informed Consent

This section confirms that written consent was obtained from all participants prior to the study.

- Ethical Approval

Eg. The paper received the ethical approval of XXX Ethics Committee.

- Trial Registration

Eg. Name of Trial Registry: Trial Registration Number

- Contributorship

The role(s) that each author undertook should be reflected in this section. This section affirms that each credited author has had a significant contribution to the article.

1. Main Manuscript

2. Reference List

3. Supplementary Data/Information

Supplementary figures, small tables, text etc.

As supplementary data/information is not copyedited/proofread, kindly ensure that the section is free from errors, and is presented clearly.

III. Abstract

A general introduction to the research topic of the paper should be provided, along with a brief summary of its main results and implications. Kindly ensure the abstract is self-contained and remains readable to a wider audience. The abstract should also be kept to a maximum of 200 words.

Authors should also include 5-8 keywords after the abstract, separated by a semi-colon, avoiding the words already used in the title of the article.

Abstract and keywords should be reflected as font size 14.

IV. Title

The title should not exceed 50 words. Authors are encouraged to keep their titles succinct and relevant.

Titles should be reflected as font size 26, and in bold type.

IV. Section Headings

Section headings, sub-headings, and sub-subheadings should be differentiated by font size.

Section Headings: Font size 22, bold type

Sub-Headings: Font size 16, bold type

Sub-Subheadings: Font size 14, bold type

Main Manuscript Outline

V. Introduction

The introduction should highlight the significance of the research conducted, in particular, in relation to current state of research in the field. A clear research objective should be conveyed within a single sentence.

VI. Methodology/Methods

In this section, the methods used to obtain the results in the paper should be clearly elucidated. This allows readers to be able to replicate the study in the future. Authors should ensure that any references made to other research or experiments should be clearly cited.

VII. Results

In this section, the results of experiments conducted should be detailed. The results should not be discussed at length in

this section. Alternatively, Results and Discussion can also be combined to a single section.

VIII. Discussion

In this section, the results of the experiments conducted can be discussed in detail. Authors should discuss the direct and indirect implications of their findings, and also discuss if the results obtain reflect the current state of research in the field. Applications for the research should be discussed in this section. Suggestions for future research can also be discussed in this section.

IX. Conclusion

This section offers closure for the paper. An effective conclusion will need to sum up the principal findings of the papers, and its implications for further research.

X. References

References should be included as a separate page from the main manuscript. For parts of the manuscript that have referenced a particular source, a superscript (ie. [x]) should be included next to the referenced text.

[x] refers to the allocated number of the source under the Reference List (eg. [1], [2], [3])

In the References section, the corresponding source should be referenced as:

[x] Author(s). Article Title [Publication Type]. Journal Name, Vol. No., Issue No.: Page numbers. (DOI number)

XI. Glossary of Publication Type

J = Journal/Magazine

M = Monograph/Book

C = (Article) Collection

D = Dissertation/Thesis

P = Patent

S = Standards

N = Newspapers

R = Reports

Kindly note that the order of appearance of the referenced source should follow its order of appearance in the main manuscript.

Graphs, Figures, Tables, and Equations

Graphs, figures and tables should be labelled closely below it and aligned to the center. Each data presentation type should be labelled as Graph, Figure, or Table, and its sequence should be in running order, separate from each other.

Equations should be aligned to the left, and numbered with in running order with its number in parenthesis (aligned right).

XII. Others

Conflicts of interest, acknowledgements, and publication ethics should also be declared in the final version of the manuscript. Instructions have been provided as its counterpart under Cover Letter.

Non-Metallic Material Science

Aims and Scope

Non-Metallic Material Science publishes original research papers, reviews, and notes that offers professional review and publication to freely disseminate research findings mainly in the areas of Polymeric Materials, Composites and Hybrid Materials, Inorganic and Carbon-based Materials. The Journal focuses on innovations of research methods at all stages and is committed to providing theoretical and practical experience for all those who are involved in these fields.

Non-Metallic Material Science aims to discover innovative methods, theories and studies in its field by publishing original articles, case studies and comprehensive reviews.

The scope of the papers in this journal includes, but is not limited to:

- Polymeric Materials
- Composites, Multi-component Materials and Hybrid Structures
- Inorganic and Carbon-based Materials
- Ceramics
- Dental Materials
- Semiconductor Materials
- Synthesis, Characterization, and Processing of Non-Metallic Materials
- Engineering Applications and Recycling of Non-Metallic Materials
- Modeling of Material Properties

Bilingual Publishing Co. (BPC)

Tel:+65 65881289

E-mail:contact@bilpublishing.com

Website:www.bilpublishing.com

About the Publisher

Bilingual Publishing Co. (BPC) is an international publisher of online, open access and scholarly peer-reviewed journals covering a wide range of academic disciplines including science, technology, medicine, engineering, education and social science. Reflecting the latest research from a broad sweep of subjects, our content is accessible world-wide—both in print and online.

BPC aims to provide an analytics as well as platform for information exchange and discussion that help organizations and professionals in advancing society for the betterment of mankind. BPC hopes to be indexed by well-known databases in order to expand its reach to the science community, and eventually grow to be a reputable publisher recognized by scholars and researchers around the world.

BPC adopts the Open Journal Systems, see on ojs.bilpublishing.com

Database Inclusion



Asia & Pacific Science
Citation Index



Creative Commons



China National Knowledge
Infrastructure



Google Scholar



Crossref



MyScienceWork



**BILINGUAL
PUBLISHING CO.**
Pioneer of Global Academia Since 1984

Tel: +65 65881289

E-mail: contact@bilpublishing.com

Website: www.bilpublishing.com

ISSN 2661-3301



9 772661 330208

Price: S\$30.00